Daniel Marcos Bonotto. International Journal of Engineering Research and Applications
www.ijera.com
ISSN: 2248-9622, Vol. 15, Issue 9, September 2025, pp 84-93

RESEARCH ARTICLE OPEN ACCESS

Comparative Study of Basaltic Rocks from Giant's Causeway, Northern Ireland, and Paraná Sedimentary Basin, Brazil

Daniel Marcos Bonotto
Geology Department, IGCE-Geosciences and Exact Sciences Institute, UNESP-São Paulo State University, Rio Claro, São Paulo State, Brazil

ABSTRACT
This paper describes a comparative study of igneous basaltic rocks occurring in two very well-known magmatic provinces: the Giant's Causeway (GC) in the northern coast of Northern Ireland, UK, and the Paraná Sedimentary Basin (PSB) in Brazil. Geochemical analysis by X-ray fluorescence was done for rock samples collected at both sites, allowing for to obtain the concentration of major oxides SiO_2, TiO_2, Al_2O_3, Na_2O, K_2O, CaO, MgO, Fe_2O_3, MnO, and P_2O_5. The results indicated that the columnar jointed basalts of the GC are low titanium (LTi) rocks (TiO_2 <2 wt.%), whereas the PSB samples are high titanium (HTi) rocks ($TiO_2 \geq 2$ wt.%). The analytical data were evaluated by some geochemical calculations and diagrams obtained from a free Excel file and software available online, which permitted differentiating the main features associated with these lava flows, for instance, a quartz supersaturation in the mineral assemblage of the HTi basaltic rocks of the PSB, relative to the GC columnar basalts.
Keywords – basaltic rocks, geochemical analysis, Giant's Causeway, Paraná Sedimentary Basin

---

Date of Submission: 01-09-2025 Date of acceptance: 09-09-2025

I. Introduction

Glass transition is a universal property of disordered materials, indicating a reversible change of solid-like and liquid-like states, typically influenced by variations in pressure, temperature, and other thermodynamic parameters. The glass transition occurs over a temperature range, although it is often referred to by a single temperature, the glass transition temperature, Tg [1].

Generally speaking, Tg is the temperature at which an amorphous material transitions from a hard, brittle, glassy state to a soft, leathery, or rubbery state, or vice versa. This reversible transition isn't a true melting point but rather a significant change in material properties, such as hardness, modulus, and elasticity, caused by chains gaining (or losing) enough energy to become more (or less) mobile [1].

The glass transition involves a significant change in the translational mobility of molecules, and it has thermodynamic characteristics of a second-order phase transition [2].

Tg is crucial for understanding and selecting materials for various applications, for instance, polymers in materials science and the food industry, among others, as it defines their mechanical behavior and operational temperature limits [2-4].

One additional very important application of this parameter is in volcanology, as magma consists of silicate melt or glass, bubbles, cracks, and crystals in varying proportions [5]. Volcanic eruptions represent one of the greatest natural hazards on Earth, as some volcanoes tend to erupt more quietly and produce lava flows, whereas others tend to erupt more violently and produce devastating density currents [6].

The ascent of magma results in drastic drops of pressure and temperature during eruption, with the exsolution or dissolution of water changing the physical and chemical properties of the magma, thus promoting or inhibiting the formation of bubbles, crystals, and cracks [5]. Anhydrous spherulitic crystals grow both above and below Tg, redistributing water into the surrounding melt [5]. Also, cracks form and are successively hydrated by magmatic water from crystal growth or by meteoric waters at temperatures lower than Tg [5].

The glass transition occurs within a temperature interval of about 100-150 °C, for most natural silicate melts at the Earth's surface, but along the cooling path of a melt from eruption (up to ~1200 °C) to the environment temperature [6].

Tg is often determined as the temperature at which the tangents to the glass and liquid curves of a given property intersect [7]. Several investigations have been conducted under controlled conditions in the laboratory to evaluate Tg considering different parameters. For instance, Richard [6] described a heat capacity (Cp) curve resulting from the first heating of a natural glass into a differential scanning calorimeter, as shown in Fig. 1. The Tg range is between the glassy state and the liquid state of the melt. The extrapolated Tg_{onset} can be used to localize the glass transition instead of Tg_{peak}, helping to identify the onset of viscous behavior for a given heating rate [6].

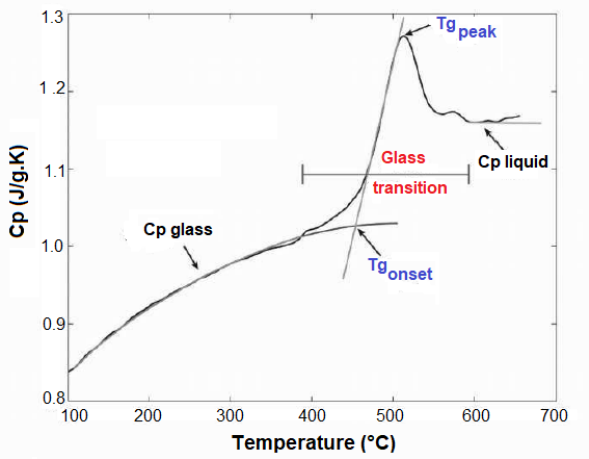

Fig. 1. Heat capacity change of a natural glass according to temperature. Adapted from [6].

Beyond changes in the physical and chemical composition of natural silicate melts at the Earth's surface associated with different Tg values, when thick lava flows cool, they tend to form hexagonal cracks, called columnar joints by geologists [8]. Upon emplacement, lava flows immediately begin to cool from the top, bottom, and sides toward the center, where the most heat remains [8]. While the bottom of the flow cools slowly because it is insulated by the ground below, the top cools more rapidly because it is exposed to the atmosphere's cooler air, wind, and rain, as well as standing or running water [8].

Among the world's best-known examples of the "columnar basalts" is the Giant's Causeway (GC) in the northern coast of Northern Ireland, lying on the edge of the Antrim plateau between Causeway Head and Benbane Head, some 40 km northeast of Londonderry [9]. There are about 40,000 basalt pillars (columns), each typically with five to seven irregular sides, jutting out of the cliff faces as if they were steps creeping into the sea [9]. However, basalt columns are a common volcanic feature, occurring on many scales and with some variations in formation, in addition to the most famous worldwide site (GC).

For instance, in India, columnars are found in several places across the volcanic traps such as the 65 Ma old Deccan Traps in South India and the 145 Ma old Rajmahal Traps in Eastern India, including other occurrences in the Indian states of Karnataka, Madhya Pradesh, Maharashtra, and Telangana [10]. In Brazil, the most famous columnar basalts occur at Pedras do Cambira [10], located in Apucarana city, northern Paraná State (Fig. 2), and are related to the Paraná Continental Flood Basalt (PCFB) province of the Paraná Sedimentary Basin (PSB), which is one of the largest igneous provinces on Earth.

Fig. 2. General view of columnar basalts occurring at Pedras do Cambira, Apucarana city, Paraná State, Brazil.

This paper describes a comparative geochemical study focusing on two important igneous provinces dominated by basaltic lavas: 1) the Antrim Plateau, which includes the GC in Northern Ireland, and 2) the PCFB in Brazil. Such provinces are characterised by huge volumes of basaltic magmas and are considered to be the products of mantle plumes or hotspots that

commonly mark the opening of major ocean basins [11].

II. Study areas and sampling

The Antrim Plateau basalts cover an area of 3500 km² in NE Ireland, where the basalts were extruded through a 30-km-thick continental crust, whose upper part is composed of Mesozoic carbonates, Palaeozoic sediments, Dalradian basement, and possibly Caledonian granites [11]. The Antrim lavas consist of about 300 m of mainly basaltic material [11], which are best known because of the spectacular columnar jointed basalts of the GC (Fig. 3). The basalts have been divided into three formations based on their distinctive petrography [12], and as well as lava flows there are numerous basaltic dykes, sills and plugs, with some of them appearing to post-date the youngest lavas [11]. Palaeomagnetic data suggested that the basalts were emplaced between 62 and 58 Ma [13], being classified as low titanium (LTi) rocks, based on the concentration of TiO_2 (<2 wt.%) as proposed by [14-17]. The GC sampling was done during an excursion to the site in July 2017 (Fig. 3).

Fig. 3. General view of LTi columnar basalts occurring at Giant's Causeway (GC) in the northern coast of Northern Ireland.

The PSB in Brazil exhibits a total surface area of about 1.6 million km² distributed as follows: 62.5% in Brazil, 25% in Argentina, 6.25% in Paraguay, and 6.25% in Uruguay [18]. The PSB is intracratonic, possessing sedimentary sequences spreading from the Silurian-Devonian times. The basin exhibits gentle dips towards the center of the basin, with the maximum thickness of sedimentary and volcanic rocks reaching up to about 8 km at the geometric center of the basin [19].

The term "Large Igneous Province" (LIP) was initially proposed by [20-22] to identify a variety of provinces composed of mafic igneous rocks that could reach > 0.1 Mkm^2 [23]. These provinces are found in oceanic and continental areas, including both volcanic and associated intrusive rocks, isolated dyke swarms, sills, and other forms of intrusions [23].

The PCFB is the sixth-largest Meso-Cenozoic LIP on Earth, occupying about 75% of the PSB area, and an estimated volume of 0.8 Mkm^3 [23]. The Serra Geral Formation (SGF) was an original designation proposed by White in 1908 for the set of basalts formed by flows in extensive fissure volcanism, to which are associated intrusive bodies of the same composition, constituting, above all, dikes and sills [24].

The main phase of magmatic manifestation occurred between 115 and 130 Ma ago, as indicated the results obtained for whole rock samples dated by the K-Ar method [25, 26]. Other estimates of the volcanism age by the ^{40}Ar-^{39}Ar method provided values between 127 and 137 Ma [27, 28], not much different from the previous ones. The duration of volcanism has been pointed out to be ~10 Ma, occurring at a low rate of 0.1 km^3/year [28].

Systematic geochemical studies of PCFB conducted by [14-17] revealed the existence of two chemically distinct rock groups (and sub-provinces) based on the TiO_2 concentration: 1) high titanium (HTi; $TiO_2 \geq 2$ wt.%), and 2) low titanium (LTi; $TiO_2 < 2$ wt.%). They are chiefly distributed, respectively, above and below the latitude 24°S [29]. Thus, the HTi group is found in the north of Paraná State, the western portion of São Paulo State, and parts of the states of Mato Grosso do Gul, Minas Gerais, and Goiás [29]. On the other hand, the LTi group spreads across the south-central part of Paraná State, the western part of Santa Catarina State, and the north of Rio Grande do Sul State [29].

The columnar basalts occurring at Pedras do Cambira are HTi (Fig. 2), in contrast to those of the GC site that are LTi (Fig. 3). HTi basaltic rocks are also widely distributed at the Corumbataí River watershed, where the UNESP Campus is located (Rio Claro city, São Paulo State), thus facilitating the sample collection for this study (Fig. 4).

Fig. 4. General view of HTi basaltic rocks of Serra Geral Formation from PSB, which were sampled at Corumbataí River watershed, São Paulo State, Brazil.

III. Experimental

One GC sample and two PSB samples were submitted to analysis in this study. The PSB samples had also been analyzed by gamma-ray spectrometry to characterize the natural radioelements U, Th and K [30]. The X-rays fluorescence (XRF) technique was utilized for the chemical analysis, which is widely used in Geosciences to provide the element concentration in samples of rocks, minerals, ores, soils, sediments, etc.

The pressed powder method was used, consisting of the mixing of about 8 g of the powdered sample (<74 μm) with ~1.5 g of a binding agent (Oregon CAS9002-88-4 wax). Then, the mix was put into a stamping machine together with 3.5-5.0 g of boric acid, yielding a pellet disc with a 40-mm diameter [31].

Two WDXRF (wavelength dispersive X-ray fluorescence) spectrometers possessing rhodium anode and installed at IGCE-UNESP-Campus de Rio Claro were used for the readings, which can separate the characteristic wavelengths with a very high degree of resolution based on optimized analyzer crystals and detectors for separating and counting the emitted X-rays [32].

The first spectrometer (S1) was used for measurements of the PSB samples, being a Philips PW 2400 machine that operates at 60 kV, 125 mA, and 3 kW of maximum voltage, current, and power, respectively. The second spectrometer (S2) was used for measurements of the GC sample, consisting of a Bruker S8 Tiger (Fig. 5) that operates at 50 kV, 50 mA, and 1 kW of maximum voltage, current, and power, respectively, but without the need for external cooling. In both spectrometers, the basic operation concept consists of a source, a sample, and a detection system, as detailed by [33, 34].

IV. Results and Discussion

The results obtained in all XRF readings are reported in Table 1. The first aspect to be highlighted from the analytical data is the confirmation that the GC sample is an LTi basaltic rock [11], while the PSB sample is an HTi one [14-17].

Niggli parameters, aiming to group the oxide components of an igneous rock according to their chemical similarity, are useful for rock characterization, rock classification, and comparison of rocks of the same or different petrographic provinces in order to determine their parental relationship and relative evolution grade [35].

Fig. 5. General view of the S8 Tiger XRF spectrometer from Bruker Co.

Table 1. Results of the XRF readings for the basaltic rock samples considered in this study. GC- Giant's Causeway. PSB-Paraná Sedimentary Basin.

Parameter	Unit	GC	PSB Sample 1	PSB Sample 2	PSB Mean
SiO_2	%	43.92	49.37	48.35	48.86
TiO_2	%	1.31	4.66	3.82	4.24
Al_2O_3	%	18.67	14.04	13.88	13.96
Na_2O	%	2.83	0.32	0.32	0.32
K_2O	%	0.60	1.93	1.59	1.76

CaO	%	11.35	8.50	10.50	9.50
MgO	%	5.63	2.31	4.45	3.38
Fe_2O_3	%	14.94	16.61	15.31	15.96
MnO	%	0.20	0.20	0.19	0.20
P_2O_5	%	0.23	0.75	0.62	0.68
SO_3	%	0.11	-	-	-
V_2O_5	%	0.05	-	-	-
SrO	%	0.05	-	-	-
CuO	%	0.03	-	-	-
ZnO	%	0.02	-	-	-
NiO	%	0.02	-	-	-
ZrO_2	ppm	73	-	-	-
Cr_2O_3	ppm	57	-	-	-
CoO	ppm	19	-	-	-

The weight percent of each oxide (WP) is used to calculate its molecular number (MN) by the equation MN = 1000 WP/MW, where MW is its corresponding molecular weight. From data reported in Table 1, four Niggli parameters are defined: 1) *al* = NM (Al_2O_3); 2) *fm* = Σ NM (FeO + MnO + MgO); 3) *c* = NM (CaO); 4) *alk* = Σ NM (Na_2O + K_2O). Then, a parameter for silica (*si*) is evaluated from the equation *si* = MN SiO_2 / (*al*+*fm*+*c*+*alk*).

Afterwards, there is a normalization step to 100, i.e., *al*+*fm*+*c*+*alk*=100. Another Niggli parameter (*si'*) is determined from comparison of the following normalized parameters:

(1) *si'*= 100+3*al*+*alk* (if *al*<*alk*)
(2) *si'*= 100+4*alk* (if *al*<*alk*+*c*)
(3) *si'*= 100 (if neither 1 nor 2 is applicable)

Finally, the quartz index (*qz*) is calculated from the difference *qz* = *si* – *si'*, implying that the rock will contain free quartz (supersaturated rock) if *qz* > 0, or that the rock will contain minerals depleted in silica, like olivine, biotite, and feldspathoids if *qz* < 0.

Table 2 shows the Niggli parameters for the basaltic rock specimens reported in Table 1. It is notorious that the *qz* value is different in both cases, i.e., *qz* is positive (higher than 0) for the HTi PSB sample, whereas it is negative (lower than 0) for the LTi GC sample. This reflects unequal magma chemical composition of the basaltic rocks analyzed, possibly also related to uneven glass transition temperature (Tg), causing a quartz supersaturation in the mineral assemblage of the HTi basaltic rocks of the PSB. Other geochemical tools also highlight differences between these basaltic specimens, as will be pointed out below.

Table 2. Niggli parameters for the rocks whose chemical composition is given in Table 1.

Parameter	GC	PSB (mean)
al	183.04	136.86
fm	330.32	286.75
c	202.68	169.64
alk	52.03	23.88
al+*fm*+*c*+*alk*	768.06	617.14
si	95.30	131.95
si'	127.08	115.48
qz	-31.78	+16.47

The AFM diagram is a ternary plot used to show the relative proportions of the oxides of alkalis (A- Na_2O+K_2O), iron (F-FeO and Fe_2O_3), and magnesium (M-MgO) in igneous rocks. The free Excel template for plotting data into the AFM diagram for igneous rocks as provided by [36] was used to plot the dataset reported in Table 1, yielding the diagram shown in Fig. 6. Both rock types exhibit a tendency of iron enrichment compared to alkalis and magnesium, thus, inserting above of the green line of Irvine and Baragar [37] and red line of Kuno [38], i.e., in the field of the subalkaline and tholeiitic rocks.

Another useful geochemical tool to identify evolution trends of basaltic rocks is the K_2O-SiO_2 diagram, in which the dataset reported in Table 1 was plotted according to the Excel template provided by [36]. Fig. 7 shows that the studied rock samples exhibit different classifications, i.e., GC belongs to the calc-alkaline series, while PSB belongs to the high-K calc-alkaline series, as defined by [39], among others.

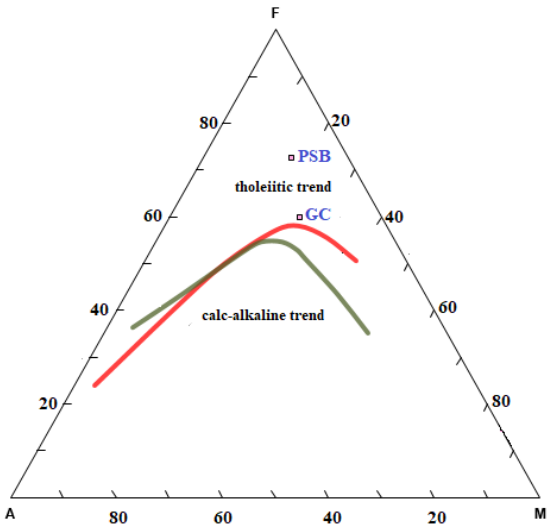

Fig. 6. AFM diagram plotting the geochemical data obtained for the GC and mean PSB basaltic rocks.

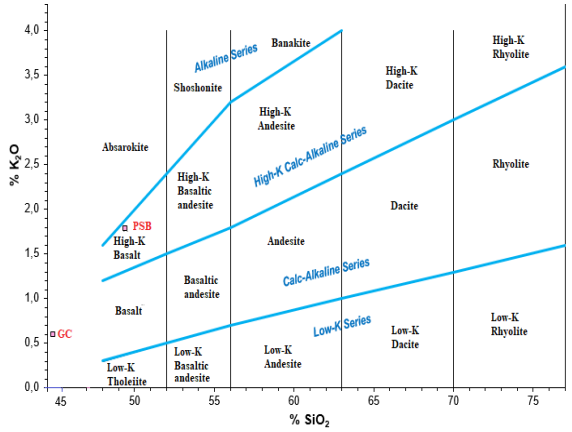

Fig. 7. K_2O-SiO_2 diagram plotting the geochemical data obtained for the GC and mean PSB basaltic rocks.

Normative analysis (NORM) corresponds to the calculation of a theoretical assemblage of standard minerals for a rock, based on the whole-rock chemical composition as determined by analytical techniques [40]. Among the various types of NORMs described in the literature, one that is often utilized is the CIPW, devised in 1931 for comparing and classifying igneous rocks, and whose name is derived from the initials of the four petrologists who proposed it (Cross, Iddings, Pirsson, and Washington).

Minetosh [41] developed a free online software to calculate the CIPW NORM, which was utilized for the dataset reported in Table 1. For the GC sample, the normative minerals are: plagioclase (60.08%), orthoclase (3.55%), diopside (11.23%), hypersthene (0.21%), olivine (6.03%), ilmenite (0.48%), hematite (14.94%), apatite (0.53%), zircon (0.01%), chromite (0.01%), and sphene (2.6%). For the mean PSB sample, the normative minerals are: quartz (19.22%), plagioclase (34.16%), orthoclase (10.4%), hypersthene (8.42%), rutile (0.8%), ilmenite (0.42%), hematite (15.96%), apatite (1.59%), and sphene (7.89%). The most relevant difference between the two mineral assemblages is the absence of quartz as a normative mineral in the GC sample, agreeing with the calculation based on the Niggli parameters, which pointed out the negative value for the *qz* index, indicative of quartz depletion/absence.

The TAS (Total Alkali-Silica) geochemical diagram has also been extensively utilized in the literature to classify volcanic rocks [42]. The dataset reported in Table 1 was plotted according to the Excel template provided by [36], yielding the graph shown in Fig. 8. Fig. 8 shows that the studied rock samples exhibit different classifications, i.e., the PSB can be classified as basalt, whilst GC as basanite (olivine>10%). A total of 59 basaltic rocks from the region of Fernandópolis (19), Jaú (14), Ribeirão Preto (21), and Franca (5) in the central-north portion of São Paulo State were analyzed by [29], with 57 being classified as basalt according to the TAS diagram and 2 as basaltic andesite. Therefore, the PSB sample analyzed in this study possesses a similar petrological classification to most rock samples reported in the investigation conducted by [29].

The IUGS Subcommission on the Systematics of Igneous Rocks was formed to review the classification and nomenclature of igneous rocks and to present proposals to IUGS. Initially, the Subcommission was concerned with plutonic rocks, suggesting the QAPF Streckeisen ternary diagram to classify the composition of silica-saturated (above; QAP) and undersaturated (below; FAP) felsic igneous rocks [43]. Afterwards, the approach has been adjusted for application to mafic (volcanic) rocks, with both possibilities incorporated into the Minetosh free online software [41], which was utilized for the dataset reported in Table 1, providing the diagram shown in Fig. 9.

Fig. 10 describes the major classification of volcanic rocks for the QAPF Streckeisen diagram illustrated in Fig. 9. Based on such nomenclature, the studied rock samples exhibit again different classification, i.e., the PSB sample is classified as dacite, whereas the GC sample as basalt/andesite.

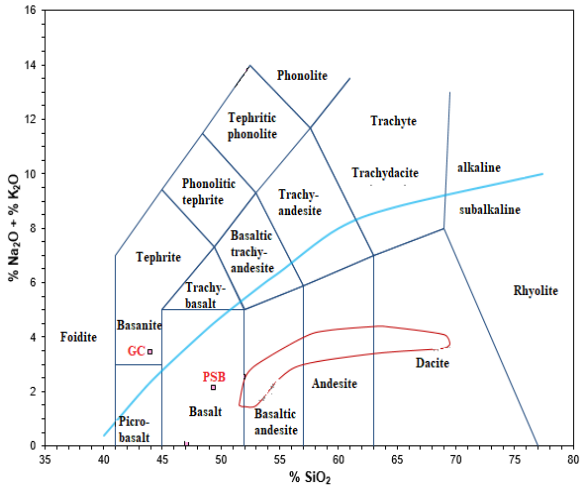

Fig. 8. TAS diagram plotting the geochemical data obtained for the GC and mean PSB basaltic rocks.

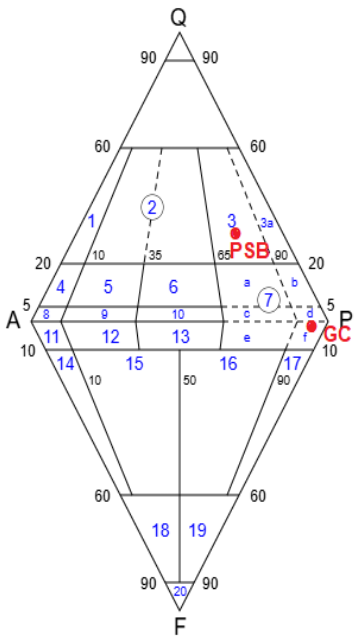

Q: The quartz content in wt% of the norm.
A: The orthoclase content in wt% of the norm.
P: The plagioclase (albite and anorthite) content in wt% of the norm.
F: The content of nepheline and leucite in wt% of the norm.

Fig. 9. QAPF Streckeisen diagram plotting the geochemical data obtained for the GC and mean PSB basaltic rocks.

INDEX	VOLCANIC ROCK
1	Quartz Alkali-Feldspar Rhyolite
2	Rhyolite
3	Dacite
4	Quartz-Bearing Alkali-Feldspar Trachyte
5	Quartz-Trachyte
6	Quartz-Latite
7	Basalt, Andesite
8	Alkali-Feldspar Trachyte
9	Trachyte
10	Latite
11	Foid-Bearing Alkali-Feldspar Trachyte
12	Foid-Bearing Trachyte
13	Foid-Bearing Latite
14	Phonolite
15	Tephritic Phonolite
16	Phonolitic Basanite
17	Basanite
18	Phonolitic Foidite
19	Tephritic Foidite
20	Foidite

Fig. 10. Types of volcanic rocks classified according to the QAPF Streckeisen diagram.

Therefore, the studied specimens of igneous rocks do not have the same classification according to the TAS and QAPG geochemical diagrams, due to the different premises involved in their construction. However, in both cases, such geochemical diagrams pointed out that the GC and PSB igneous rocks are related to lava flows exhibiting diverse chemical composition. In view of the large number of "columnar basalts" occurring worldwide, promising approaches are encouraged to be developed for improving the knowledge associated with the volcanic emissions.

V. Conclusion

Volcanic systems are very complex, involving the use of several tools to obtain a deeper understanding and relationships of the parameters involved, such as the magma composition, volatile content, cooling rate, viscosity, and temperature at which the amorphous soft, leathery, or rubbery material transitions to a hard, brittle, and glassy state. Predicting eruptions and evaluating their associated hazard is a great challenge nowadays to mitigate catastrophic events caused by violent, devastating lava flows. This study focused on two important volcanic areas associated with igneous basaltic rocks, identifying similarities and differences between them by the use of geochemical data, which allowed determine the Niggli parameters and normative minerals (NORM), as well as its plotting in the AFM, K_2O-SiO_2, TAS, and QAPF Streckeisen diagrams. The first igneous occurrence corresponded to the Giant's Causeway in Northern Ireland, UK, which exhibited low TiO_2 concentration (<2 wt.%), negative quartz index, absence of quartz as a normative mineral, insertion in the group of rocks belonging to the calc-alkaline series, and classification as basanite (olivine>10%) or basalt/andesite. The second igneous occurrence corresponded to samples providing from the Paraná Sedimentary Basin in Brazil Giant's, which exhibited high TiO_2 concentration (>2 wt.%), positive quartz index, presence of quartz as a normative mineral, insertion in the group of rocks belonging to the high-K calc-alkaline series, and classification as basalt or dacite. Despite such differences, both rock types exhibited a tendency of iron enrichment compared to alkalis and magnesium, helping on the development of further investigations focusing equivalent igneous rocks occurring elsewhere.

Acknowledgements

CNPq (Brazilian National Council for Scientific and Technological Development) for Grant No. 304010/2021-9. Gabrielle R. Ceccato for X-ray fluorescence analysis of the GC sample.

REFERENCES

[1] ScienceDirect, *Glass Transition.* [https://www.sciencedirect.com/topics/materials-science/glass-transition] Accessed 30 August 2025.

[2] Y.H. Roos, Mapping the different states of food components using state diagrams, in Y.S. Kasapis, I.T. Norton, and J.B. Ubbink (Eds.) *Modern Biopolymer Science*, (Cambridge, MA: Academic Press, 2009) 261-276.

[3] Y. Wang, and T. Truong, Glass transition and crystallization in foods, in B. Bhandari, and Y.H. Roos (Eds.) *Non-equilibrium states and glass transitions in foods: Processing effects and product-specific implications*, (Sawston, UK: Woodhead Publishing, 2017) 153-172.

[4] S. Ebnesajjad, Introduction to plastics, in E. Baur, K. Ruhrberg, and W. Woishnis (Eds.) *Chemical resistance of commodity thermoplastics*, (Amsterdam: Elsevier, 2016) xiii-xxv.

[5] F.W. von Aulock, *Bubbles, crystals and cracks in cooling magma*, PhD Thesis. (University of Canterbury, Canterbury, UK, 2013).

[6] D. Richard, *Crossing the glass transition during volcanic eruptions: A matter of time scale and magma rheology*, Dissertation. (University of Munich, Munich, Germany, 2015).

[7] B. Mysen, and P. Richet, Glass versus Melt, in B. Mysen, and P. Richet (Eds.) *Silicate glasses and melts*, 2nd edn. (Amsterdam: Elsevier, 2019) 39-75.

[8] HVO (Hawaiian Volcano Observatory-USGS), *Volcano Watch – Columnar jointing provides clues to cooling history of lava flows*. [https://www.usgs.gov/observatories/hvo/news/volcano-watch-columnar-jointing-provides-clues-cooling-history-lava-flows] Accessed 30 August 2025.

[9] Wikipedia, *Giant's Causeway*. [https://en.wikipedia.org/wiki/Giant%27s_Causeway] Accessed 30 August 2025.

[10] Wikipedia, *List of places with columnar jointed volcanics*. [https://en.wikipedia.org/wiki/List_of_places_with_columnar_jointed_volcanics] Accessed 30 August 2025.

[11] J.A. Barrat, and R.W. Nesbitt, Geochemistry of the Tertiary volcanism of Northern Ireland, *Chemical Geology*, *129*, 1996, 15-38.

[12] R.A. Old, The age and field relationships of the Tardree Tertiary rhyolite complex, County Antrim, N. Ireland, *Bulletin of the Geological Survey Great Britain*, *51*, 1975, 21-40.

[13] A.E. Mussett, Timing and duration of activity in the British Tertiary Igneous Province, in A.C. Morton, and L.M. Parson (Eds.) *Early Tertiary Volcanism and the Opening of the NE Atlantic*, (Geol. Soc. London, Spec. Publ., 1988) 337-348.

[14] G. Bellieni, E.M. Piccirillo, and B. Zannetin, Classification and nomenclature of basalts, *USGS Commission on the Systematics of Igneous Rocks*, *circ. 34*, 1981, 1-17.

[15] G. Bellieni, P. Brotzu, P. Comin-Chiaramonti, M. Ernesto, A.J. Melfi, I.G. Pacca, E.M. Piccirillo, and D. Stolfa, Petrological and palaeomagnetic data on the plateau basalts to rhyolite sequencies of the Southern Paraná Basin (Brazil), *Anais da Academia Brasileira de Ciências*, *55*, 1983, 355-383.

[16] G. Bellieni, P. Comin-Chiaramonti, L.S. Marques, A.J. Melfi, E.M. Piccirillo, A.J.R. Nardy, and A. Roisenberg, High- and low-Ti flood basalts from the Paraná plateau (Brazil): petrology and geochemical aspects bearing on their mantle origin, *Neues Jahrbuch für Mineralogie Abhandlungen*, *150*, 1984, 272-306.

[17] G. Bellieni, P. Comin-Chiaramonti, L.S. Marques, A.J. Melfi, A.J.R. Nardy, C. Papatrechas, E.M. Piccirillo, A. Roisenberg, and D. Stolfa, Petrogenetic aspects of acid and basaltic lavas from Paraná plateau (Brazil): geological, mineralogical and petrochemical relationships, *Journal of Petrology*, *27*, 1986, 915-944.

[18] L.M. Araújo, A.B. Franca, and P.E. Potter, Hydrogeology of the Mercosul aquifer system in the Paraná and Chaco-Paraná Basins, South America, and comparison with the Navajo-Nugget aquifer system, USA, *Hydrogeology Journal*, *7*, 1999, 317-336.

[19] P. Zalán, S. Wolff, J. Conceição, I.S. Vieira, V.T. Appi, and O.A.P. Zanotto, Tectonics and sedimentation at Paraná basin, *Proc. Brazilian Southern Geological Symposium*, Curitiba, PR, 1987, 441-477. (in Portuguese)

[20] M.F. Coffin, and O. Eldholm, Large igneous provinces, *Scientific American*, *269*, 1993, 42-49.

[21] M.F. Coffin, and O. Eldholm, Scratching the surface: estimating dimensions of large igneous provinces, *Geology*, *21*, 1993, 515-518.

[22] M.F. Coffin, and O. Eldholm, Large igneous provinces: crustal structure, dimensions, and external consequences. *Review of Geophysics*, *32*, 1994, 1-36.

[23] F.B. Machado, E.R.V. Rocha-Júnior, L.S. Marques, A.J.R. Nardy, L.V. Zezzo, and N.S. Marteleto, Geochemistry of the Northern Paraná Continental Flood Basalt (PCFB) Province: implications for regional chemostratigraphy. *Brazilian Journal of Geology*, *48* (2), 2018, 177-199.

[24] F.F.M. Almeida, and M.S. Melo, Paraná basin and Mesozoic volcanism, in IPT (São Paulo State Technological Research Institute) (Ed.) *Geological map of São Paulo State*, 1. (São Paulo: Promocet, 1981) 46-81. (in Portuguese)

[25] A.J. Melfi, Potassium-argon ages for core samples of basaltic rocks from southern Brazil, *Geochimica et Cosmochimica Acta*, *31*, 1967, 1079-1089.

[26] G. Amaral, U.G. Cordani, K. Kawashita, and J.H. Reynolds, Potassium-argon dates of basaltic rocks from southern Brazil, *Geochimica et Cosmochimica Acta*, *30*, 1966, 159-189.

[27] P.R. Renne, M. Ernesto, I.G. Pacca, R.S. Coe, J.M. Glen, M. Prévot, and M. Perrin, The age of Paraná flood volcanism, rifting of Gondwanaland, and the Jurassic-Cretaceous boundary, *Science*, *258*, 1992, 975-979.

[28] S. Turner, M. Regelous, S. Kelley, C.J. Hawkesworth, and M.S.M. Mantovani, Magmatism and continental break-up in the South Atlantic: high precision ^{40}Ar-^{39}Ar geochronology, *Earth and Planetary Science Lett*ers, *121*, 1994, 333-348.

[29] E. Squisato, A.J.R. Nardy, F.B. Machado, L.S. Marques, E.R.V. Rocha Júnior, and M.A.F. Oliveira, Lithogeochemistry and petrogenetic aspects of basalts from the Paraná magmatic province in the north-central portion of the state of São Paulo, *Geosciences*, *28* (1), 2009, 27-41. (in Portuguese)

[30] F.T. da Conceição, and D.M. Bonotto, Radiometric dose exposition and composition of sedimentary and igneous rocks from Corumbataí River basin (SP), *Brazilian Journal of Geophysics*, *24* (1), 2006, 37-48. (in Portuguese)

[31] G. Roveratti, and D.M. Bonotto, XRF analysis applied to the Batateira River Formation (Araripe Sedimentary Basin, Ceará State, Brazil), in S. Brookes (Ed.) *Sedimentary basins: Evolution, methods of formation and recent advances* (New York, USA: Nova Science, 2018), 75-99.

[32] B. Beckhoff, B. Kanngießer, N. Langhoff, R. Wedell, and H. Wolff, *Handbook of practical X-ray fluorescence analysis* (Springer, New York, 2005).

[33] D.M. Bonotto, and G. Roveratti, Comparative geochemical analysis by XRF of sediments for limnological studies, in B. Veress, and J. Szigethy (Eds.) *Horizons in Earth Sciences Research,* v. 20 (New York, USA: Nova Science, 2020), 41-64.

[34] G. Roveratti, and D.M. Bonotto, End-user procedure for the calibration of an X-rays fluorescence spectrometer, in J.C. Taylor (Ed.) *Advances in Chemistry Research* (New York, USA: Nova Science, 2017), 231-247.

[35] R.H. Mitchell, and S.C. Bergman, *Petrology of lamproites* (Plenum Press, New York, 1991).

[36] H.G. Stosch, *TAS diagram, K_2O-SiO_2 diagram and AFM diagram template for Excel*. [https://zenodo.org/records/5977826] Accessed 30 August 2025.

[37] T.N. Irvine, and W.R.A. Baragar, A guide to the chemical classification of the common volcanic rocks, *Canadian Journal of Earth Sciences*, *8*, 1971, 523-548.

[38] H. Kuno, Differentiation of basalt magmas, in H.H. Hess, and A. Poldervaart (Eds.) *Basalts: The Poldervaart Treatise on Rocks of Basaltic Composition*, v. 2 (New York, USA: Interscience, 1968) 623-688.

[39] A. Peccerillo, and S.R. Taylor, Geochemistry of Eocene calc-alkaline volcanic rocks from the Kastamonu area, northern Turkey, *Contributions to Mineralogy and Petrology*, *58*, 1976, 63-81.

[40] S. Dutch, *The CIPW Norm*. [https://academic.sun.ac.za/natural/geology/undergraduate/G314/G314-06-Prac2-Calculating%20CIPW%20 norms.pdf] Accessed 30 August 2025.

[41] Minetosh online, *CPIW-norm calculation*. [https://minetoshsoft.com/cipw/cipwcalc.html] Accessed 30 August 2025.

[42] M.J. Le Bas, R.W. Le Maitre, A. Streckeisen, and B. Zanettin, A chemical classification of volcanic rocks based on the total alkali-silica diagram, *Journal of Petrology*, *27*, 1986, 745-750.

[43] A. Streckeisen, Classification and Nomenclature of Plutonic Rocks Recommendations of the IUGS Subcommission on the Systematics of Igneous Rocks, *Geologische Rundschau*, *63*, 1974, 773-786.